THE JOURNAL OF PHYSICAL CHEMISTRY Letters

Cite This: J. Phys. Chem. Lett. 2018, 9, 5207−5212

Letter

pubs.acs.org/JPCL

Observation of Singlet Oxygen with Single-Molecule Photosensitization by Time-Dependent Photon Statistics

Yao Li, Ruiyun Chen, Haitao Zhou, Ying Shi, Chengbing Qin, Yajun Gao, Guofeng Zhang, Yan Gao, Liantuan Xiao,* and Suotang Jia

State Key Laboratory of Quantum Optics and Quantum Optics Devices, Institute of Laser Spectroscopy, Shanxi University, Taiyuan 030006, China

Collaborative Innovation Center of Extreme Optics, Shanxi University, Taiyuan, Shanxi 030006, China

Supporting Information

ABSTRACT: The singlet oxygen has been widely applied to the treatment of physiological diseases, and the photosensitized generation of singlet oxygen is the main means of its physiological applications. On the basis of the fluctuation of fluorescence field from single photosensitizer, we characterize the generation of singlet oxygen at single molecule level with the time-dependent photon statistical method. By measuring the time-tagged-time-resolved single-molecule fluorescence photons, we analyze the time-dependent Mandel-Q parameter, which has been performed at different oxygen environment. It is shown that the single molecule not only offers an efficient way of generating singlet oxygen in ambient condition but also provides insights for the fluctuation of singlet oxygen in the nanoscale environment. The method of time-dependent photon statistics provides a convenient methodology for observing photosensitizers generating singlet oxygen in real time at single photosensitizer level.

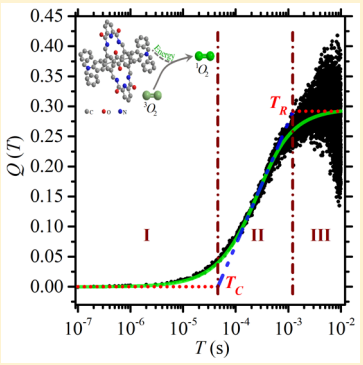

Singlet oxygen ($^1O_2$) is widely involved in physiology, pharmacology, bioscience, especially in the metabolism of many living organisms.[1−4] It is also shown as an important substance in photodynamic cancer therapy.[5−7] In the physiological condition, the generation of singlet oxygen is mainly originating from the interaction of photosensitizers with laser and triplet oxygen ($^3O_2$), where the photosensitizers in their triplet state will exchange energy with triplet oxygen and thus lead the formation of singlet oxygen.[2,8−12] The generation of singlet oxygen under different conditions have been reported recently, such as singlet oxygen generation via energy transfer in nanocomposites based on semiconductor quantum dots and porphyrin ligands[13] and microenvironment-switchable singlet oxygen generation by axially coordinated hydrophilic ruthenium phthalocyanine dendrimers,[10] as well as the control of singlet oxygen generation photosensitized by *meso*-anthrylporphyrin through interaction with DNA.[14] As a kind of photosensitizers, fluorescent dye molecules have an important role in the life sciences due to their nondestructive way of tracking and/or analyzing biological molecules through fluorescence imaging. In particular, as dye molecules label to a diseased tissue or cell to generate singlet oxygen, they can treat damaged cells at a specific site, which has broad application prospects in physiology and medicine.[2]

To apply singlet oxygen in physiology, their detection has great significance. In particular, in the photodynamic therapy of cancer cells and skin diseases, the efficiency of singlet oxygen generation on drugs is a crucial indicator to characterize the therapeutic effect of drugs on diseased cells.[15,16] Actually, singlet oxygen can be identified by electron paramagnetic resonance or phosphorescence characteristics itself.[17−19] These methods can determine the amount of singlet oxygen well. However, some limitations, such as complicated equipment, long measurement period, and strong signal requirements, restrict the characterization of singlet oxygen in many areas. Above all, the generation and detection of singlet oxygen at single molecule level is quite difficult, considering the low generation rate of singlet oxygen via energy transfer with one photosensitizer. However, these techniques have important applications in physiology and medicine, such as getting insight into the mechanism of therapy by singlet oxygen at single molecule level.

In this work, we present a method to observe the generation of singlet oxygen at single molecule level by characterizing the fluorescence properties of single photosensitizer. The generation of singlet oxygen is achieved by energy transfer between triplet state single photosensitizer and triplet oxygen,[8,9,20,21] which will substantially vary the relax processes of triplet state and thus change the fluorescence fluctuation properties of single photosensitizer.[22−24] Here we characterize the fluorescence fluctuation of single photosensitizer by time-dependent Mandel-Q parameter ($Q(T)$),[22,25] without the necessary to define an arbitrary threshold between on- and off-levels. The Mandel-Q parameter of single photosensitizer at different time scale have been investigated to determine its

Received: July 4, 2018
Accepted: August 14, 2018
Published: August 20, 2018

DOI: 10.1021/acs.jpclett.8b02088
J. Phys. Chem. Lett. 2018, 9, 5207−5212

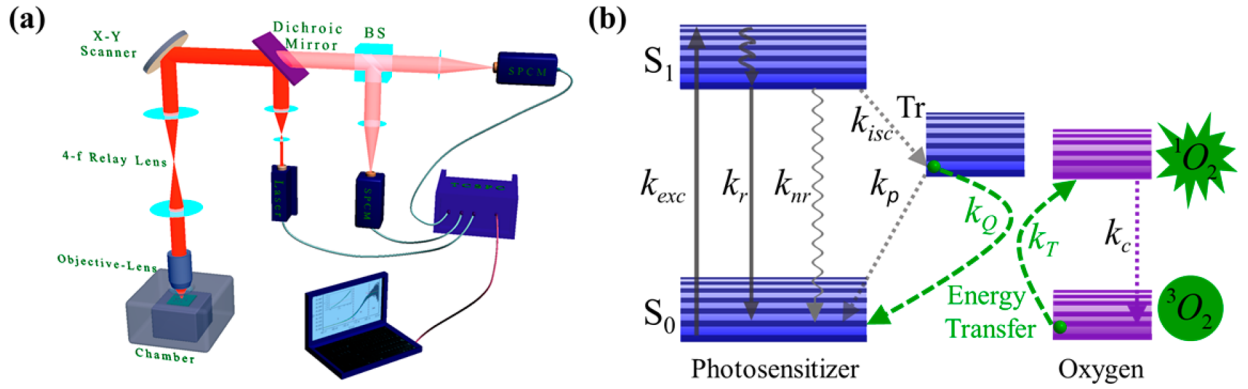

Figure 1. (a) Confocal scanning fluorescence imaging microscopy with a time-correlated single-photon counting (TCSPC) module. (b) Scheme of energy levels and interactions between SR molecule and oxygen. k_{exc}, k_r, and k_{nr} are the rates of excitation, radiation, and nonradiative relaxation, respectively. k_{isc} is the rate of intersystem crossing, k_p is the rate of Tr state returns to S_0, and k_c is the rate of phosphorescence of $^1O_2$. k_Q and k_T are the rates of exchange energy between Tr state of single molecule and triplet oxygen.

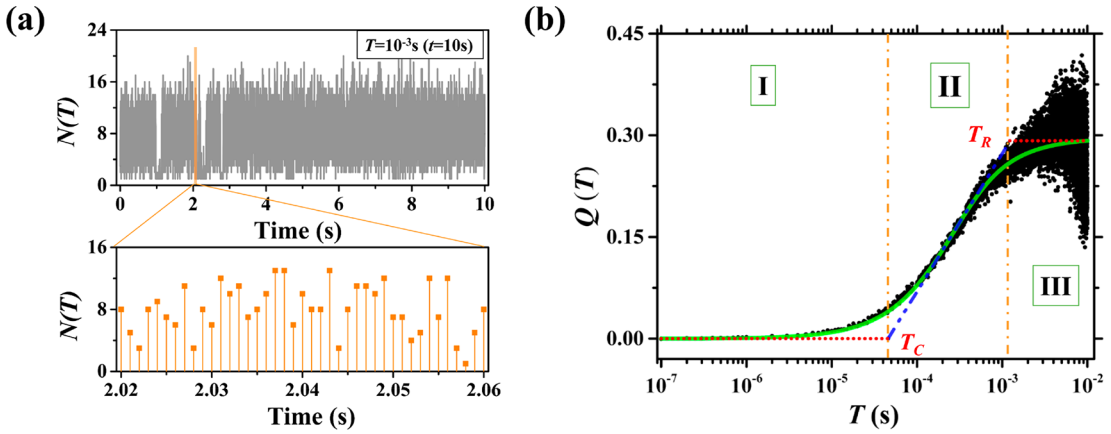

Figure 2. Time-dependent Mandel-Q parameter ($Q(T)$) of a SR molecule. (a) Sequences of $N(T)$ as T equaling to 10^{-3} s. (b) The black points are the $Q(T)$ values of SR molecule obtained at various time scales, and the green solid line is obtained by fitting the $Q(T)$ curve with eq 2. The blue and red dashed lines are three characteristic tangents of the $Q(T)$ curve, with the two intersections (T_C and T_R) dividing the $Q(T)$ curve into three parts, labeled as I, II, and III, respectively.

characteristic features and reveal the fluctuation of fluorescence field. The characteristic features varied as the concentration of triplet oxygen have been studied. The results indicate that this time-dependent photon statistical method can quantitatively analyze the generation of singlet oxygen on the single-molecule fluorescence-field in real time.

To explore the generation of singlet oxygen, Figure 1b presents the mechanism of energy transfer between SR molecules and oxygen. The ground state SR molecules (S_0) can be excited to their first excited state (S_1) by the pulsed laser with the rate of k_{exc}. The electron in excited state can relax by three channels: returning to S_0 by the radiative recombination (emitting a fluorescence photon) with the rate of k_r (4.5×10^8 s^{-1}, the detailed derivation of the rates involving with energy transfer can be found in the third section of Supporting Information) and/or the nonradiative process with the rate of k_{nr}, as well as transferring to triplet state (Tr) by intersystem crossing with rate of k_{isc} (5×10^7 s^{-1}). Then, the electron will further return to S_0 from Tr with the rate of k_p (5×10^2 s^{-1}). When the electron cycles between S_1 and S_0 states, the SR molecule will continuously emit fluorescent photons and thus its fluorescence-field will remain very stable. When the electron transfers to the Tr state, the fluorescence emission will be interrupted for a period of time since the rate of k_p is small. This intrinsic intermittent of fluorescence emission will increase the fluctuation of the fluorescence field. In contrast, when the triplet oxygen approaches a single SR molecule, the SR may return to S_0 from Tr by energy transfer with triplet oxygen at the rate of k_Q (2.6×10^4 s^{-1}). As a consequent, the triplet oxygen will excite to singlet oxygen with the rate of k_T. In this process, the SR acts as the photosensitizer, triplet oxygen acts as the quencher of Tr state. Considering the k_Q is almost 2 orders of magnitude larger than k_p, triplet oxygen will primarily exchange energy with SR molecules to generate the singlet oxygen as it approaches SR molecules. When the triplet oxygen is present, the electron will return to S_0 quickly (due to the large k_Q), and the rapid cycle between S_0 and S_1 will be establish, resulting in the stable fluorescence emission. When the triplet oxygen is absent, the electron will stay in the Tr state for a long time (due to the small k_p), and the fluorescence of the SR molecule will alternate between the on-state and off-state, resulting in obvious fluctuation of the fluorescence field. Therefore, by measuring the fluctuation of fluorescence field, the concentration of triplet oxygen and the generation of singlet oxygen can be observed in real time.

Generally, the fluctuation of fluorescence field can be reflected by the properties of emitted photons $N(T)$ in a period of time T, as shown in Figure 2a (detailed procedure to

DOI: 10.1021/acs.jpclett.8b02088
J. Phys. Chem. Lett. 2018, 9, 5207−5212

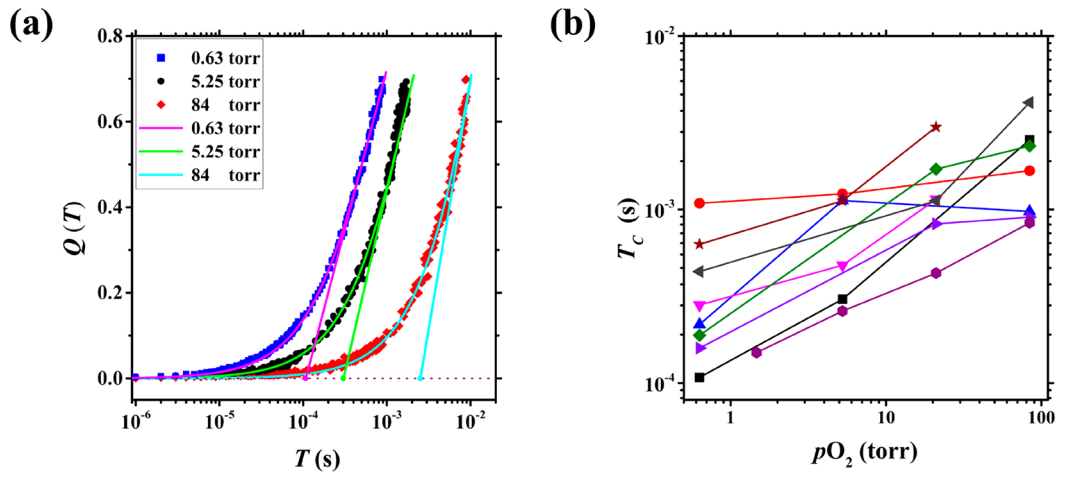

Figure 3. Oxygen-dependent T_C for single SR molecule. (a) The solid dots with three different shapes in the figure are experimental date (different shapes correspond to different pO_2), and the solid curve is obtained by fitting the $Q(T)$ to eq 2, taking the intersection of the tangents of the fitting curves to get the T_C, and mark them as solid dots. (b) T_C of nine molecules at different pO_2, which determines the rate of singlet oxygen generation (each color represents the T_C of one molecule in different oxygen concentrations).

generate $N(T)$ from the raw data can be found in the first section of the Supporting Information). To quantitatively describe the fluorescence fluctuation features of single SR molecules induced by triplet oxygen, we evaluate the $Q(T)$ of the fluorescence field from single molecule, which can be expressed as[22,27,28]

$$Q(T) = \frac{\langle(\Delta N(T))^2\rangle}{\langle N(T)\rangle} - 1 \tag{1}$$

Here angle brackets can be understood as a mean value in the same period of time T, $\langle(\Delta N(T))^2\rangle$ is the variance of $N(T)$. Taking T equaling to 10^{-3} s as an example, the fluorescence trajectory will be divided into 10^4 (t/T, here t is the total measurement time. As shown in Figure 2a, t is equal to 10 s for this trajectory). The number for each part can be obtained by counting the emitted photons from the TCSPC data acquisition card (Figure S1). Then $\langle N(T)\rangle$ and $\langle(\Delta N(T))^2\rangle$ can be calculated from these 10^4 numbers. Consequently, $Q(10^{-3})$ is determined (setailed procedure to generate $Q(T)-T$ graph can also be found in the first section of the Supporting Information). When $Q(T) = 0$, the fluorescence field has a Poissionian distribution, while when $Q(T) > 0$, it has a super-Poissionian distribution.[25,27,29,30] Figure 2b presents a typical $Q(T)$ for a SR molecule. It can be found that at the time scale smaller than 10^{-5} s, $Q(T)$ almost equals zero, indicating the Poissionian distribution of fluorescence emission. When the time scale is larger than 10^{-5} s, $Q(T)$ increases rapidly and shows a super-Poissionian behavior. This is due to the direct impact of the Tr state, which results in the switch of single-molecule fluorescence intensity between on-state and off-state.

For single molecule system, the $Q(T)$ curve can be fitted by the model considering the intermittency of fluorescence field:[27]

$$Q(k\tau_{rep}) = \frac{2P_{ISC}}{\beta^2}\left\{1 - \frac{1}{k\beta}[1 - (1-\beta)^k]\right\} - 1 \tag{2}$$

where $\beta \equiv P_{ISC} + q\tau_{rep}$, P_{ISC} is the intersystem crossing probability per excitation pulse, and $q = k_p + k_Q$, which is the rate of electrons returning to S_0 from Tr, τ_{rep} is time interval between laser pulse, k is the number of pulses. As the green solid line shown in Figure 2b, the fitted result agrees well with the experimental data. To get insight into the fluctuation features of fluorescence field, we defined two characteristic statistics parameters, T_C and T_R, in the $Q(T)$ curve. These two values are determined by the crossing points of three tangent lines, which are the tangent to the fitted curve at the start and end points with the convergent values less than 10^{-2}, as well as the point with the largest first derivative (Detailed determination has been presented in Figure S2 in the Supporting Information). Thus, the fluorescence fluctuation features of single SR molecule can be divided into three time scales by T_C and T_R, as shown in Figure 2b. Region I, with time scale less than the time of electrons returning to S_0 from Tr, describes the fluctuation of the fluorescence of single molecule in its on-state. Region II, with time scale in the vicinity of the time of electrons returning to S_0 from Tr, presents the fluorescence-field of the single SR molecule entering the super-Poisson distribution. Region III, however, describes the influence of the longer-time off-state, which is induced by the cationic state that dominates the dynamics of SR molecule on a larger time scale.[31,32]

The present of triplet oxygen and the generation rate of singlet oxygen will substantially reduce the time of electrons returning to S_0 from Tr (due to the large k_Q), thus will significantly vary the time scale of fluorescence from SR molecule entering the super-Poisson distribution, *i.e.*, T_C. To verify this hypothesis, we collect the fluorescence emission of a same single SR molecule at different oxygen partial pressures (pO_2) and calculate the $Q(T)$ curves, as shown in Figure 3a. Note that the higher the pO_2, the larger time scale the $Q(T)$ curve entering the super-Poissonian distribution. This phenomenon clearly reveals that the value of T_C is strongly dependent on the concentration of triplet oxygen and the generation rate of singlet oxygen. On the other word, T_C can be used as an indicator to characterize the generation of singlet oxygen. To eliminate the anisotropy of single molecule, we also perform the oxygen concentration dependent T_C for different single SR molecules, as shown in Figure 3(b). Note that most of the molecules show similar trend as that in Figure 3a, which is larger T_C at higher oxygen concentrations. In other word,

DOI: 10.1021/acs.jpclett.8b02088
J. Phys. Chem. Lett. 2018, 9, 5207−5212

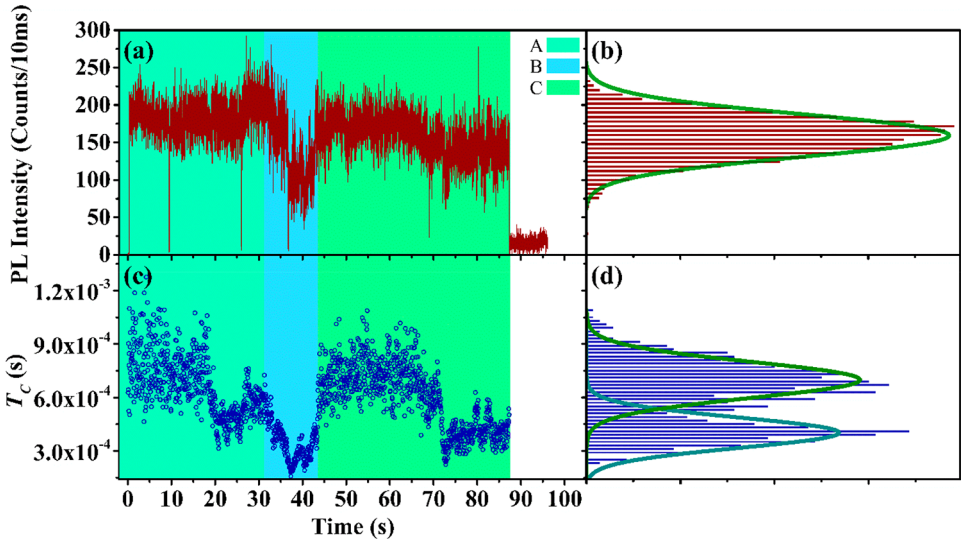

Figure 4. Trajectory of the fluorescence intensity and T_C for one SR molecule at 1.26 Torr of pO_2. (a) The red line is the fluorescence trajectory and (b) its corresponding statistical intensity distribution for the area C with Gaussian fitted line. (c) The blue circles show the trajectory of the T_C for the molecule and its statistical distribution for area C in part (d), and the solid line is the double Gaussian fitting of its statistical distribution.

more singlet oxygen is generated by SR molecule at higher oxygen concentrations. However, few of the SR molecules as the blue curve "▲" shown in Figure 3(b), presents the decrease of T_C when the pO_2 increases. These unexpected changes can be understood as the nonuniform dynamic characteristics of oxygen molecules in the nanoenvironment. (As shown in Figure S6, the statistical distribution of T_C of more than 200 SR molecules under different oxygen concentration has been provided as the further evidence to eliminate the anisotropy of single molecules.)

By measuring the fluorescence fluctuation features of individual molecule based on time-dependent photon statistics, we can not only detect the change of oxygen concentration, but also monitor the fluctuation of oxygen in nanoenvironment and the generation of singlet oxygen. (As a comparison experiment, the photon statics results without significant change under different pressures of pure Nitrogen have been presented in Figure S7 in Supporting Information.) Figure 4a shows the fluorescence intensity trajectory of the SR molecule at pO_2 of 1.26 Torr and the corresponding T_C trajectory in the Figure 4c. Note that T_C presents clearly two levels, one is larger than 6.0×10^{-4} s with major fluctuation, and the other is smaller than 6.0×10^{-4} s with minor fluctuation. The statistical distribution for the area C can be fitted by a double Gaussian distribution, as shown in Figure 4d. These two levels hint the interaction and noninteraction of single SR molecule with triplet oxygen. Here the larger T_C can be used as the indicator to observe the generation of singlet oxygen. Note that although the fluorescence intensity and T_C synchronously decrease in area B, however, there is no obvious change in the fluorescence intensity in the area A and C, and the histogram of fluorescence intensity can be well fitted with a single Gaussian function in the Figure 4b. This phenomenon suggests that T_C can reveal the fluctuation of singlet oxygen generation at single molecule level that is unclear by detecting fluorescence trajectory.

In conclusion, we present a time-dependent photon statistical method to monitor the generation of singlet oxygen at the single-molecule level. This method is realized based on the energy transfer between the photosensitizer of single SR molecule and triplet oxygen, which will vary the fluctuation of fluorescence filed of SR molecule. We use the time-dependent Mandel-Q parameter to describe the features of fluorescence filed at the single-molecule level, and define characteristic parameter T_C to indicate the generation of singlet oxygen. T_C varied as oxygen concentration and measurement time have been investigated, suggesting that our method can be used to monitor the generation of single oxygen at single-molecule level in real time. Our method will provide a new approach to elaborate the mechanism of therapy by singlet oxygen in physiology at single-molecule level.

■ EXPERIMENTAL SECTION

Here, the squaraine-derived rotaxane (SR, 1001, Molecular Targeting Technologies, Inc.) molecules were used as the photosensitizer to generate the singlet oxygen, in view of its high efficiency energy transfer with triplet oxygen.[26] The single molecule sample was prepared by spin-coating 20 μL solution (dissolved in dimethysulfoxide) containing 10^{-10}–10^{-9} mol. SR molecules onto the glass coverslip at 2500 rmp. The concentration of SR molecules was kept at such a low level that either one molecule or no molecule was in the focus. As shown in Figure 1a, the prepared sample was mounted in a chamber (Montana Instruments) for measurement. The concentration of triplet oxygen was controlled by changing the pressure of the chamber from 727 to 0.3 Torr. The chamber filled with pure nitrogen has also been performed, as a comparison experiment. The fluorescence field of single SR molecule was investigated by combining a home-built confocal scanning fluorescence microscope with a time-correlated single-photon counting (TCSPC) data acquisition card (HydraHarp 400, PicoQuant). A 385 fs pulsed fiber laser (Toptica, FemtoFiber Pro) with a repetition rate of 10 MHz and the central wavelength of 635 nm was used to excite SR molecules. As shown in Figure 1a, the laser was reflected by a dichroic mirror and a 4-*f* telecentric relay lens system with a fast steering scanner (Newport, FSM-300-M-03), and finally focused by an objective lens (Olympus, LUCPFLN60x, NA = 0.7) onto the sample. The fluorescence photons were collected by the same objective, separated by a beam splitter (BS) and focused on

DOI: 10.1021/acs.jpclett.8b02088
J. Phys. Chem. Lett. 2018, 9, 5207–5212

two single-photon counting modules (SPCM, τ−SPAD-50, PicoQuant). Laser synchronization signal and the absolutely arrived time of each photon were recorded by using the time-tagged-time-resolved (TTTR) mode of the TCSPC data acquisition card.

■ ASSOCIATED CONTENT

Supporting Information

The Supporting Information is available free of charge on the ACS Publications website at DOI: 10.1021/acs.jpclett.8b02088.

Introduction to the acquisition of $N(T)$ and $Q(T)-T$ graph, the determination of T_C and T_R, the photophysical properties of SR molecule, and the photon statistics of SR molecules under different oxygen concentration and pure nitrogen atmosphere (PDF)

■ AUTHOR INFORMATION

Corresponding Author

*(L.X.). E-Mail: xlt@sxu.edu.cn. Telephone:+86-0351-7113-805. Fax: +86-0351-7113-863.

ORCID

Yao Li: 0000-0002-0187-4733

Haitao Zhou: 0000-0001-5325-5275

Chengbing Qin: 0000-0002-6822-5113

Guofeng Zhang: 0000-0002-9030-0431

Notes

The authors declare no competing financial interest.

■ ACKNOWLEDGMENTS

We acknowledge the funding from the National Key Research and Development Program of China (No. 2017YFA0304203), the National Natural Science Foundation of China (Nos. 61527824, 11504216, 61675119, U1510133, 61605104, and 11434007), PCSIRT (No. IRT13076), and 1331KSC.

■ REFERENCES

(1) To, T.-L.; Fadul, M. J.; Shu, X. Singlet Oxygen Triplet Energy Transfer Based Imaging Technology for Mapping Protein-Protein Proximity in Intact Cells. *Nat. Commun.* **2014**, *5*, 4072.

(2) Ogilby, P. R. Singlet Oxygen: There Is Indeed Something New under the Sun. *Chem. Soc. Rev.* **2010**, *39*, 3181−3209.

(3) Preuss, A.; Chen, K.; Hackbarth, S.; Wacker, M.; Langer, K.; Roeder, B. Photosensitizer Loaded Hsa Nanoparticles Ii: In Vitro Investigations. *Int. J. Pharm.* **2011**, *404*, 308−316.

(4) Torring, T.; Helmig, S.; Ogilby, P. R.; Gothelf, K. V. Singlet Oxygen in DNA Nanotechnology. *Acc. Chem. Res.* **2014**, *47*, 1799−1806.

(5) Turan, I. S.; Gunaydin, G.; Ayan, S.; Akkaya, E. U. Molecular Demultiplexer as a Terminator Automaton. *Nat. Commun.* **2018**, *9*, 805.

(6) Ragas, X.; He, X.; Agut, M.; Roxo-Rosa, M.; Gonsalves, A. R.; Serra, A. C.; Nonell, S. Singlet Oxygen in Antimicrobial Photodynamic Therapy: Photosensitizer-Dependent Production and Decay in E. Coli. *Molecules* **2013**, *18*, 2712−2725.

(7) Clement, S.; Deng, W.; Camilleri, E.; Wilson, B. C.; Goldys, E. M. X-Ray Induced Singlet Oxygen Generation by Nanoparticle-Photosensitizer Conjugates for Photodynamic Therapy: Determination of Singlet Oxygen Quantum Yield. *Sci. Rep.* **2016**, *6*, 19954.

(8) Bai, S.; Barbatti, M. Spatial Factors for Triplet Fusion Reaction of Singlet Oxygen Photosensitization. *J. Phys. Chem. Lett.* **2017**, *8*, 5456−5460.

(9) Filatov, M. A.; Baluschev, S.; Landfester, K. Protection of Densely Populated Excited Triplet State Ensembles against Deactivation by Molecular Oxygen. *Chem. Soc. Rev.* **2016**, *45*, 4668−4689.

(10) Hahn, U.; Setaro, F.; Ragas, X.; Gray-Weale, A.; Nonell, S.; Torres, T. Microenvironment-Switchable Singlet Oxygen Generation by Axially-Coordinated Hydrophilic Ruthenium Phthalocyanine Dendrimers. *Phys. Chem. Chem. Phys.* **2011**, *13*, 3385−3393.

(11) Hirakawa, K.; Hirano, T.; Nishimura, Y.; Arai, T.; Nosaka, Y. Dynamics of Singlet Oxygen Generation by DNA-Binding Photosensitizers. *J. Phys. Chem. B* **2012**, *116*, 3037−3044.

(12) Mosinger, J.; Lang, K.; Hostomsky, J.; Franc, J.; Sykora, J.; Hof, M.; Kubat, P. Singlet Oxygen Imaging in Polymeric Nanofibers by Delayed Fluorescence. *J. Phys. Chem. B* **2010**, *114*, 15773−15779.

(13) Zenkevich, E. I.; Sagun, E. I.; Knyukshto, V. N.; Stasheuski, A. S.; Galievsky, V. A.; Stupak, A. P.; Blaudeck, T.; von Borczyskowski, C. Quantitative Analysis of Singlet Oxygen ($^1O_2$) Generation Via Energy Transfer in Nanocomposites Based on Semiconductor Quantum Dots and Porphyrin Ligands. *J. Phys. Chem. C* **2011**, *115*, 21535−21545.

(14) Hirakawa, K.; Hirano, T.; Nishimura, Y.; Arai, T.; Nosaka, Y. Control of Singlet Oxygen Generation Photosensitized by Meso-Anthrylporphyrin through Interaction with DNA. *Photochem. Photobiol.* **2011**, *87*, 833−839.

(15) Zhao, T.; et al. Gold Nanorod Enhanced Two-Photon Excitation Fluorescence of Photosensitizers for Two-Photon Imaging and Photodynamic Therapy. *ACS Appl. Mater. Interfaces* **2014**, *6*, 2700−2708.

(16) Ghogare, A. A.; Greer, A. Using Singlet Oxygen to Synthesize Natural Products and Drugs. *Chem. Rev.* **2016**, *116*, 9994−10034.

(17) Laine, M.; Barbosa, N. A.; Kochel, A.; Osiecka, B.; Szewczyk, G.; Sarna, T.; Ziolkowski, P.; Wieczorek, R.; Filarowski, A. Synthesis, Structural, Spectroscopic, Computational and Cytotoxic Studies of Bodipy Dyes. *Sens. Actuators, B* **2017**, *238*, 548−555.

(18) Mano, C. M.; et al. Excited Singlet Molecular O_2 ($^1\Delta_g$) Is Generated Enzymatically from Excited Carbonyls in the Dark. *Sci. Rep.* **2014**, *4*, 5938.

(19) Zadlo, A.; Szewczyk, G.; Sarna, M.; Kozinska, A.; Pilat, A.; Kaczara, P.; Sarna, T. Photoaging of Retinal Pigment Epithelial Melanosomes: The Effect of Photobleaching on Morphology and Reactivity of the Pigment Granules. *Free Radical Biol. Med.* **2016**, *97*, 320−329.

(20) Wu, Y.; Zhen, Y.; Ma, Y.; Zheng, R.; Wang, Z.; Fu, H. Exceptional Intersystem Crossing in Di(Perylene Bisimide)S: A Structural Platform toward Photosensitizers for Singlet Oxygen Generation. *J. Phys. Chem. Lett.* **2010**, *1*, 2499−2502.

(21) Ashwood, B.; Jockusch, S.; Crespo-Hernandez, C. E. Photochemical Reactivity of Dtpt3: A Crucial Nucleobase Derivative in the Development of Semisynthetic Organisms. *J. Phys. Chem. Lett.* **2017**, *8*, 2387−2392.

(22) Sanchez-Andres, A.; Chen, Y.; Muller, J. D. Molecular Brightness Determined from a Generalized Form of Mandel's Q-Parameter. *Biophys. J.* **2005**, *89*, 3531−3547.

(23) Mitsui, M.; Unno, A.; Azechi, S. Understanding Photoinduced Charge Transfer Dynamics of Single Perylenediimide Dyes in a Polymer Matrix by Bin-Time Dependence of Their Fluorescence Blinking Statistics. *J. Phys. Chem. C* **2016**, *120*, 15070−15081.

(24) Verberk, R.; van Oijen, A. M.; Orrit, M. Simple Model for the Power-Law Blinking of Single Semiconductor Nanocrystals. *Phys. Rev. B: Condens. Matter Mater. Phys.* **2002**, *66*, 233202.

(25) Barkai, E.; Jung, Y.; Silbey, R. Theory of Single-Molecule Spectroscopy: Beyond the Ensemble Average. *Annu. Rev. Phys. Chem.* **2004**, *55*, 457−507.

(26) Xiao, S.; Fu, N.; Peckham, K.; Smith, B. D. Efficient Synthesis of Fluorescent Squaraine Rotaxane Dendrimers. *Org. Lett.* **2010**, *12*, 140−143.

(27) Treussart, F.; Alleaume, R.; Le Floc'h, V.; Xiao, L. T.; Courty, J. M.; Roch, J. F. Direct Measurement of the Photon Statistics of a Triggered Single Photon Source. *Phys. Rev. Lett.* **2002**, *89*, 093601.

DOI: 10.1021/acs.jpclett.8b02088
J. Phys. Chem. Lett. 2018, 9, 5207−5212

(28) Zheng, Y. J.; Brown, F. L. H. Single Molecule Photon Emission Statistics in the Slow Modulation Limit. *J. Chem. Phys.* **2004**, *121*, 7914−7925.
(29) Bel, G.; Zheng, Y.; Brown, F. L. H. Single Molecule Photon Counting Statistics for Quantum Mechanical Chromophore Dynamics. *J. Phys. Chem. B* **2006**, *110*, 19066−19082.
(30) Zheng, Y. J.; Brown, F. L. H. Single Molecule Photon Emission Statistics for Non-Markovian Blinking Models. *J. Chem. Phys.* **2004**, *121*, 3238−3252.
(31) Haase, M.; Hubner, C. G.; Reuther, E.; Herrmann, A.; Mullen, K.; Basche, T. Exponential and Power-Law Kinetics in Single-Molecule Fluorescence Intermittency. *J. Phys. Chem. B* **2004**, *108*, 10445−10450.
(32) Zondervan, R.; Kulzer, F.; Orlinskii, S. B.; Orrit, M. Photoblinking of Rhodamine 6g in Poly(Vinyl Alcohol): Radical Dark State Formed through the Triplet. *J. Phys. Chem. A* **2003**, *107*, 6770−6776.

DOI: 10.1021/acs.jpclett.8b02088
J. Phys. Chem. Lett. 2018, 9, 5207−5212